Journal of the Korean Physical Society, Vol. 52, No. 3, March 2008, pp. 639∼648

Single-Particle Tracking Method for Quantitative Tracking and Biophysical Studies of the MinE Protein

U. Junthorn, S. Unai, P. Kanthang, W. Ngamsaad and C. Modchang
R&D Group of Biological and Environmental Physics, Department of Physics, Faculty of Science, Mahidol University, Bangkok 10400, Thailand

W. Triampo*
R&D Group of Biological and Environmental Physics, Department of Physics, Faculty of Science, Mahidol University, Bangkok 10400, Thailand and Center of Excellence for Vector and Vector-Borne Diseases, Faculty of Science, Mahidol University, Nakhonpathom 10400, Thailand

C. Krittanai
Institute of Molecular Biology and Genetics, Mahidol University, Nakhonpathom 73170, Thailand

D. Wtriampo
Department of Chemistry, Faculty of Science, Mahidol University, Bangkok 10400, Thailand

Y. Lenbury
Department of Mathematics, Faculty of Science, Mahidol University, Bangkok 10400, Thailand

(Received 4 October 2007)

The dynamics of the MinE protein has been recognized to play an important role in accurate placement of the septum during cell division. The system is of great interest because it represents one of the few biologically self-sustaining oscillatory systems in an organism that can be well-studied at physical, generic and biochemical levels. In this work, single-particle tracking (SPT) was, for the first time, applied to investigate the MinE behavior in an *E. coli* system. The SPT data monitored from the dividing *E. coli* cells, 5.08 ± 0.82 μm in length, have demonstrated an oscillation of the MinE protein between the two poles with an average period of 266.64 ± 122.29 seconds. The results for the oscillating trajectory and velocity can be classified according to the space and time scales of dynamic events into two types: flight events and switching events. The switching events mostly occur near polar zones while the flight events take place between the switching events in the space between the polar zones. From quantitative analysis, we found the flight events to occur with an average flight velocity of 0.23 ± 0.08 μm/s and the flight events to occur during turning at the poles with an average switching velocity of 2.16 ± 0.68 μm/s. The agreements between our findings and those from previous studies are discussed. These results demonstrate the benefits of applying SPT to investigate the oscillations of targeted proteins in both qualitative and quantitative ways. The emphasis of this report is not on discovering biophysical information but on providing a new methodology to obtain information that will be essential to evaluate the many mathematical models that have been proposed to account for the Min protein oscillation system.

PACS numbers: 87.15.He, 87.17.Ee
Keywords: Single- particle tracking, *E. coli*, Cell division, Min proteins, MinE, Protein oscillation

I. INTRODUCTION

Despite many years of investigation, the mechanism of cytokinesis in cells, even in bacteria, remains not thoroughly understood. Specifically in Escherichia coli (*E. coli*) and other rod-shaped bacteria, cell division normally occurs at the midpoint of the long axis of the cell and depends on the precise placement (less than 1 % of deviation [1]) of a division septum at the middle of the cell. This process is initiated by the assembly of an equatorial ring (Z-ring) of the tubulin-like FtsZ GTPase on the cytoplasmic membrane [2,3] The Z-ring assembly is spatially restricted to midcell by nucleoid occlusion [4,

*E-mail: scwtr@mahidol.ac.th; wtriampo@gmail.com

5] and by the dynamics of the Min protein system [6,7]. The nucleoid-free zones provide possible placement of Z-ring with three regions, two polar zones and a midcell zone, while the Min protein system prevents Z-ring assembly at the polar zone, leaving just the midcell zone as the only possibility. With these crucial roles of the Min protein system, here, the dynamics of the Min system, specifically the MinE protein, is our main concern.

The Min system consists of MinC, MinD and MinE expressed from the *minB* operon [6], which restricts separation to the desired potential division site at the midcell through the oscillatory cycle from pole to pole [8]. Normally, MinC co-localizes and co-oscillates with MinD [9,10] which act together as a negative regulator of Z-ring assembly and their oscillatory dynamics depends on MinE [9–11]. The MinCD complex prevents the correct interaction of FtsA with the FtsZ ring *in vivo* [12] and MinC has been shown to inhibit FtsZ polymerization *in vitro* [9]. Thus, inhibition of polar division seems to be achieved by transiently disrupting assembly of the division machinery at each cell pole in an alternating manner. In addition, oscillation and, therefore, topological specificity depends on the MinE protein, which was shown to form a dynamic ring that appears to "sweep" the MinCD protein off the membrane into the cytoplasm. After entering the cytoplasm, MinCD then appears to reassemble at the opposite cell pole [13,14]. In this process, ATPase activity is required and is also strongly influenced by the concentration of MinD. MinD ATPase activity can be stimulated by MinE *in vitro*.

Generally, proteins can be labeled and tracked with fluorescent particles or latex beads. The discovery and development of green fluorescent protein (GFP) from the jellyfish *Aequorea victoria* have revolutionized our ability to study protein localization dynamics and interactions in living cells [15,16]. In so doing, these fluorescent proteins have allowed protein function to be investigated within the complex environment of the cell. Paralleling the developments in GFP biology has been advances in fluorescence imaging methods and microscope systems that make it easy to visualize the localization of GFP fusion proteins, to quantify their abundance and to probe their mobility and interactions. Imaging methods such as fluorescence recovery after photobleaching (FRAP), fluorescence resonance energy transfer (FRET) and fluorescence correlation spectroscopy (FCS) have been modified so that they can be done on user-friendly, commercially available, laser scanning microscopes, replacing the need for custom-built microscopes. However, the signal or obtained information only reflects the cluster behavior that typically is too coarse to reveal dynamic information on an individual molecule. Therefore, an alternative approach is adopted, namely, a single-particle tracking (SPT) technique.

The SPT is a computer-enhanced video microscopy that has been developed to measure not only the movement of single small molecules or particles but also the trajectory of molecule ensembles [17,18]. Mostly, it is used to track the motion of proteins or lipids on the cell surface, individual molecules, or small clusters with a typical spatial resolution of tens of nanometers and a typical time resolution of tens of milliseconds. The SPT has been used mostly in data analysis in order to classify the modes of motion (*e.g.*, normal diffusion, anomalous diffusion, confined motion, *etc.*) and to find the distribution of quantities characterizing the motion. When compared with, perhaps, more well-known techniques, namely fluorescence recovery after photobleaching (FRAP), the major advantage of SPT over FRAP is the possibility that the movement of molecules can be characterized with a much higher spatial resolution, nanometers instead of microns. Thus, fewer assumptions on the movement of the particles themselves should be made in order to gain the maximum information from their trajectories. As mentioned earlier, the data from SPT measurements generally constitute an important key for characterizing cell membranes. Hence, it not only is a probe of membrane microstructure but can also contribute significantly to the study of reaction kinetics within the cell membrane. The SPT technique has been used in many fields of biophysical research, such as in plasma and nuclear membrane studies [18], nuclear trafficking of viral genes [19], chromosome dynamics [20] and bacterial actin motion [21].

On the study of the Min protein system, most works have experimentally focused on assembly and dynamics especially related to the spatial-temporal pattern formation and periods of the MinCDE system. An excellent review is given by Lutkenhaus [22]. In terms of technique-based approaches, the majority of the works has used fluorescent proteins with selectively labeled single proteins, together with high-resolution fluorescence imaging, which is made possible by a new generation of bright-field and confocal microscopes [7,9,11,14,23–25]. Of particular interest is the work by de Boer and co-workers [6] who studied the localization of MinD by monitoring a membrane-associated protein of MinD in fixed *E. coli* cells. With immunoelectron microscopy, anti-MinD antiserum and colloidal gold-labeled second antibody were used to reveal MinD associated with the cytoplasmic membrane [26]. However, most results were only qualitatively good. Precise GFP-MinD or GFP-MinE data in terms of positions, velocities, trajectories and so on, are still not good enough. In fact, these data are still very rare, mainly because reliable position tracking, data processing and analysis software are still not well known among the researchers in this particular field. If the positions in time series of Min proteins (provided by GFP-Min protein signals) are to be tracked precisely, the following conditions must be met: 1) the image capturing CCD must be fast enough, 2) the stages or samples must be stable enough to prevent frame shift at a small length scale, 3) the noise or thermal fluctuation is not very large and 4) the fluorescent signal lasts consistently long enough to retain reasonable data. Otherwise, the interpretation could be wrong and not reproducible.

Motivated by the above-mentioned considerations, this work has been devoted to the adaptation of this SPT technique for a quantitative study of Min protein dynamics. To the best of our knowledge, this is the first time ever that the SPT technique has been applied to this MinE dynamics problem. The focus is on the dynamics of assembly and localization of MinE protein oscillations. As shall be seen later, our results will confirm all previous qualitative results and can be used to provide, for example, the characteristic timescale, the reaction rate, the diffusion coefficient and so on. With regards to Min protein dynamics both *in vitro* and *in silico*, a considerable number of experiments have been done. Computationally, several studies have been carried out with different reaction-diffusion models to explain these oscillations [13,14,27]. Hence, with regards to Min protein dynamics, not only can the qualitative information be obtained with this SPT technique but also more direct quantitative information may be obtained, as well. This allows us to more precisely and specifically answer the crucial questions associated with these phenomena. For example, how do particles move on the cell surface? How are the proteins assembled? Therefore, our results can potentially bridge the gap between the *in silico* and the *in vitro* or *in vivo* experiments.

II. MATERIALS AND METHODS

1. Bacterial Strain and Growth Conditions

E. coli strain RC1/pSY1083G [$\Delta min/\mathrm{P}_{lac} - \Delta minC$ $minD$ $minE$ :: gfp] was kindly provided by Yu-Ling Shih (Department of Microbiology, University of Connecticut Health Center) [24]. For expression of MinE labeled with green fluorescent proteins (GFP), a starter of RC1/pSY1083G cells was grown in LB medium, 50 μg/ml ampilcillin, 25 % glucose at 37 °C and 250 rpm shaking overnight. Then, 1 % of the overnight culture was taken to grow in the new medium until the $\mathrm{OD}_{600\ \mathrm{nm}}$ was approximately $0.3 - 0.4$. The centrifugation was performed at 3,000 rpm for 15 min to collect the cells. Cells were then re-suspended for at least 30 min in the same medium containing 0.1 mM isopropyl-β-D-thiogalactopyranoside (IPTG) for protein induction. The cell culture was diluted with media before use. In our experimental preparation, $5 - 7$ μl of the sample was dropped on a glass slide coated with 5 μl of poly-L-lysine (0.1 %), which was then covered by a cover slip at room temperature (25 °C) before examination.

2. Image Acquisition

The fluorescence image sequences were performed with the Zeiss Axioskop2 and Nikon TE2000E fluorescence microscopes with 100X oil lenses. An additional 1.5 time magnification was made to the images of the Nikon microscope. Images were collected at 1 frame/second by using a charge-coupled device (CCD) camera (Model Revolution$^{\mathrm{TM}}$ QEI Camera Monochrome) and an InVivo software support in exposure times of 900 ms.

3. Image Processing and SPT

The single-particle tracking (SPT) technique [17,18] is used to follow the region of interest (ROI), which gives the highest GFP:MinE concentration signal. This highest intensity is a representation of MinE cluster in the cell. The data obtained from the SPT measurements are supported by SpotTracker Java plugin of public domain ImageJ software (*SpotTracker: Single particle tracking over noisy images sequence:* Available at http://bigwww.epfl.ch/sage/soft/spottracker/SpotTracker ImageJ software: Available at http://rsb.info.nih.gov/ij/). The SpotTracker is a fast and robust computational procedure to track fluorescent particles attached to a molecule of interest in time-lapse microscopy. The tracking process was performed in steps as follows:

First, the *E. coli* cell length in the raw fluorescence image sequence was rotated to be along the major axis (x-axis). The goal for rotating the *E. coli* cell to be along the major axis was to make it simple for image analysis because the protein behavior of the MinE oscillation is along the cell length. Second, because the acquired image sequence was high in noise resulting from thermal fluctuations and fading of the fluorescence signals (typically about $4 - 5$ minutes after activating the fluorescence), at this stage the final image sequence was noisy. This effect could reduce the accuracy of the GFP:MinE positions collected from SpotTracker or lead to misinterpretation of the GFP:MinE phenomenon, so the noisy images obtained were further processed using a Gaussian filter with 2-pixel radius in order to reduce the effect of noise. It should be noted that if the pixel radius is too large, the positions of the ROI would not be accurate. Third, the signal-to-noise ratio was enhanced by using the rescaling option of the SpotTracker plugin. Then, the tracking procedure of the ROI was performed using again the SpotTracker plugin. With this tracking, we were finally provided with time series data on the position of the ROI of the GFP:MinE system in text file (x, y) coordinates. Lastly, the positions of MinE were analyzed by using MATLAB software to calculate the physical quantities, including trajectory, velocity, period and probability distribution. In fact, other dynamic quantities could also be calculated via this method. More details of this tracking in time algorithm can be found in Ref. 19.

III. RESULTS AND DISCUSSIONS

Proteins are dynamic systems. They localize to specific environments (*i.e.*, membranes, cytosol, organelle

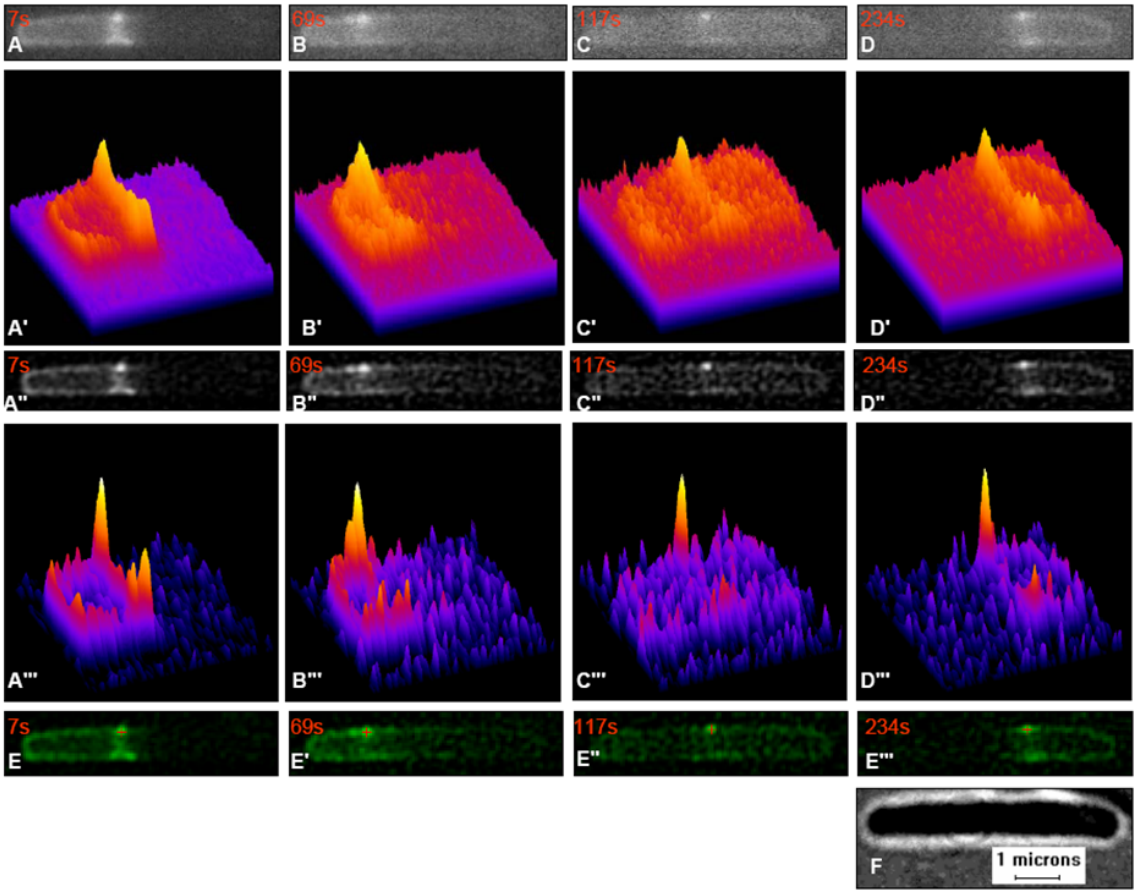

Fig. 1. Image processing and SPT results for RC1/pSY1083G [$\Delta min/P_{lac} - \Delta minC\Delta minD\Delta minE :: gfp$]. Figures 1(A), (B), (C) and (D) show raw fluorescence images at times 7 s, 69 s, 117 s and 234 s. Figures 1(A$'$), (B$'$), (C$'$) and (D$'$) are intensity plots of fluorescence images corresponding to the high-intensity clusters of the raw image in Figures 1(A), (B) and (C), respectively. Figures. 1(A$''$), (B$''$), (C$''$) and (D$''$) show the results of images after filtering the Gaussian option from ImageJ and the rescaling option from the SpotTracker plugin that corresponds to the intensity plots in Figures 1(A$'''$), (B$'''$), (C$'''$) and (D$'''$) (fourth row from above). Figures 1(E), (E$'$), (E$''$) and (E$'''$) show the results of fluorescence images with green and red plus sign after high-intensity tracking in the same time interval. Figures 1(F) shows a differential interference contrast (DIC) image showing an $\sim$5.5-μm cell length.

lumen, or nucleoplasm), undergo diffusive or directed movement and often have mechanical parts, the actions of which are coupled to chemical events. The fine tuning of geography, movement and chemistry gives proteins their extraordinary capability to regulate virtually all dynamic processes in living cells. Protein motions are essential for function. It is reasonable to say that the mechanism for the functionality of protein molecules can be elucidated by knowledge of molecular conformations and their dynamics.

Here, we have applied the SPT technique to experimentally and quantitatively investigate the dynamics of a MinE protein assembly and its movement. With a combination of the SPT technique and image processing, we were able to demonstrate a redistribution pattern of MinE. In order to study this dynamic behavior of MinE protein molecules, we traced their moving positions the high-intensity region.

Figure 1 shows an image sequence of MinE:GFP before and after image processing, as well as SPT products. The use of the Gaussian option from ImageJ, together with the rescaling and the tracking options from the SpotTracker plugin, results in more improved images and spotted spatial coordinates. Figures 1(A)-(D) show raw fluorescence images at times 7s, 69s, 117s and 234s, respectively. Figures 1(A$''$)-(D$''$) show the results of images after applying the noise-filter Gaussian option from ImageJ and the rescaling option from SpotTracker plugin. After that, the high intensity spot from the tracking product was performed in the red plus sign shown in Figures 1(E)-(E$'''$). For better understanding, Figure 1(F) shows a DIC micrograph (gray), $\sim$5.5 μm of cell length. From this SPT measurement, the x and the y coordinates of the center of the ROI are provided and the sequence of positions (x, y), as obtained at successive times, will be used to study the MinE dynamics. Figures 1(A$'$)-(D$'$) are intensity plots of fluorescence images corresponding to the high-intensity clusters in the images

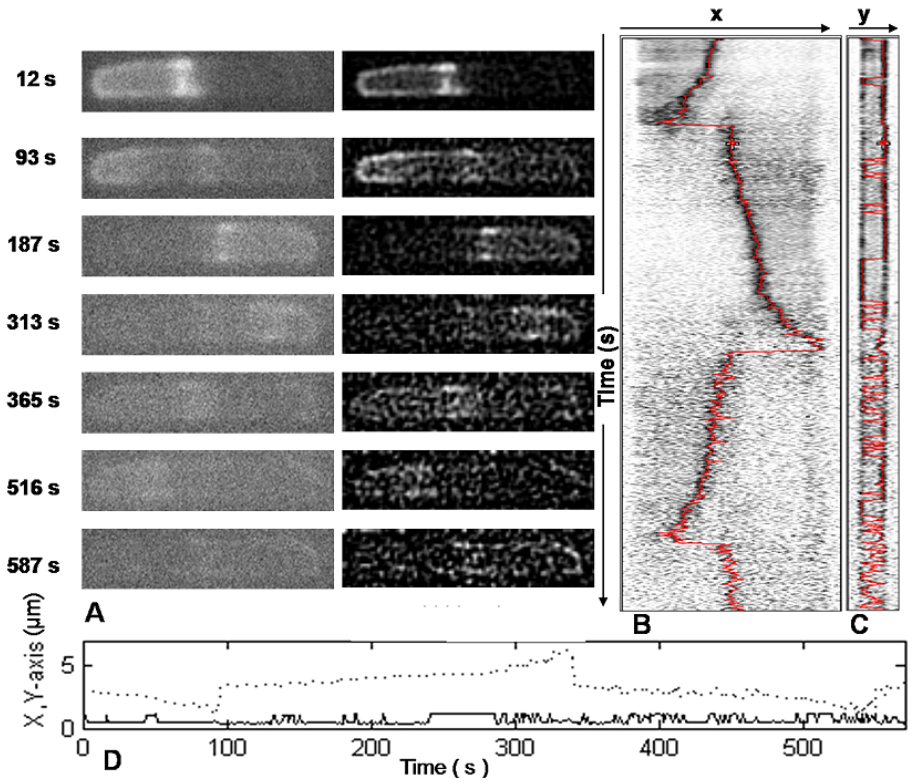

Fig. 2. The raw time-lapse and enhanced 2D-image sequence of MinE oscillations at different times corresponding to a product of the SpotTracker plugin. Figures 2(A) shows the 2D image sequence of MinE oscillations at different times. The first column exhibits the raw fluorescence image sequence and the next column represents the product of the signal enhancement of the image sequence from the SpotTracker plugin. Each fluorescent image sequence shows a small cluster of GFP:MinE as a bright color that moves from midcell to the polar zone and backward near the midcell displayed in first three rows. A product from SpotTracker plugin is shown in Figure 2(B) and the red line corresponds to a GFP signal trajectory of MinE oscillations on $x(t)$ axis. Similarly, as shown in Figure 2(C), the red line on $y(t)$ axis is the spot projection exhibiting the GFP signal trajectory. Figure 2(D) is time evolution plots of the positions on the $x(t)$ axis as a dash line and on the $y(t)$ axis as a solid line.

in Figures 1(A)-(D) while Figures 1(A‴)-(D‴) are the image sequence as a result of image processing by means of filtering Gaussian option from ImageJ and the rescaling option from the SpotTracker plugin. From these intensity plots, as seen, the fire-shade peak indicates the high intensity of the GFP signals which relate to the local concentration of the MinE proteins. On comparing Figures 1(A′)-(D′) with Figures 1(A‴)-(D‴), it is quite evident that the noises are considerably decreased, as clearly marked by red sprinkles being distributed much less in Figures 1(A‴)-(D‴). This, consequently, highlights the location of the fire-shaded peaks, which gives the main contribution to the precisely tracked spots of MinE.

In order to demonstrate how to extract the trajectory profiled from the SPT process, Figure 2(A) portrays once again a time series of images before (left) and after (right) the SpotTracker plugin was used. It should be remarked that as a result of noise elimination and image enhancement, the spotted signals (white spots), which represent the MinE accumulation at that moment, are more greatly pronounced. Moreover, it allows us to clearly see (12 s – 93 s) the GFP:MinEs "flow" from at/near the midcell to the left edge around the polar zone and immediately back to the midcell area. This evidence is confirmed by the fact that MinE proteins mostly accumulate at the cell center [28]. In a similar manner, the subsequent data show the "flow" of protein signals, but in the opposite direction. This phenomenon appears to be cyclic, which may be driven by the concentration gradients of the MinE protein and by a more complicated mechanism, which may actively require energy for the cell. In addition, this event may be supported by the theory of the C-terminal functioning as the topological specificity of MinE proteins [29]. For a more quantitative view, in Figure 2(B) and Figure 2(C), the red lines indicate a MinE:GFP signal trajectory of MinE oscillations on the $x(t)$ and the $y(t)$ axes, respectively. The re-plot of these trajectories as a time evolution of positions along the x axis (dashed line) and the y axis (solid line) are shown in Figure 2(D).

Figure 3 shows the analyzed time evolution of the distance and the velocity during 570th time step. In Figure 3(A), the displacement $R = \sqrt{(\Delta x)^2 + (\Delta y)^2}$ man-

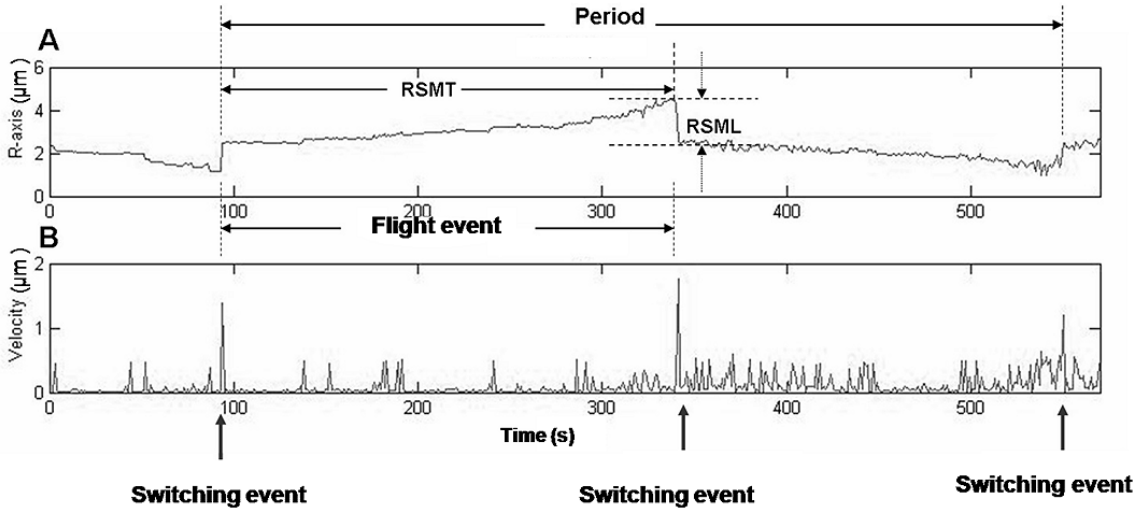

Fig. 3. Comparison between the distance and the velocity time-evolutions during 570 seconds. Figure 3(A) exhibits a time evolution plot of R ($\sqrt{(\Delta x)^2 + (\Delta y)^2}$). The ring-structure moving time (RSMT) indicates the time from midcell to the polar zone and the ring- structure moving length (RSML) indicates the distance of GFP:MinE moving from the polar zone to the midcell. An oscillation period (∼456 seconds for this cell sample) is the measurement of three switching velocities or three switching events as peaks shown in Figure 3(B). The black arrows under Figure 2(B) indicate switching events, including the switching velocity and RSML. Events in which GFP:MinE get trapped between two switching events are called flight events and include the flight velocity and RSMT (details are given the text).

ifestly designates the periodic-like pattern. The amplitude called, *the ring-structure moving length (RSML)*, indicates the displacement from midcell to the polar zones and its corresponding time, *the ring-structure moving time (RSMT)*. This apparently demonstrates that GFP:MinE proteins typically take relatively long times to move from the midcell to the poles (∼227.50 seconds) while they take relatively much shorter times (∼1 − 3 seconds) to switch form the pole back to the midcell. Consequently, high concentrations of GFP:MinE are typically found in the midcell regions. From length and time scales, we classify the characteristics of GFP:MinE protein dynamics according to the space and time scales of the dynamic events into two types: *flight event* and *switching event*.

Flight events feature the movement between the midcell and poles, which include the flight velocity and the RSMT, as shown Figures 3(A) and (B). The flight velocity is the GFP:MinE lateral movement from midcell to the polar zones. The mall peaks of velocities that occur between switching events show that GFP:MinE jumps from side to side along the y-axis, as presented in Figure 3(B). Our measurement of the flight velocity yields 0.23 ± 0.08 μm/s for 7 individual cells. This phenomenon reflects E-ring structure movement in which MinE proteins form as E-ring structure at the mid-region to activate the ATPase activity of MinD:ATP molecules to undergo hydrolysis. This results in the release of the MinD:ADP, MinC and MinE products from the membrane to the cytoplasm [8, 30–32]. The RSMT is the time spent while GFP:MinE laterally moves from midcell to the polar zone, which corresponds to the oscillation period. On average, the RSMT was calculated to be ∼133.25 seconds which is approximately half of the oscillation period (266.64 ± 122.29 seconds).

Flight events correspond to the return from the pole back to the midcell, including the switching velocity and the RSML, as shown in Figures 3(A) and (B). The switching velocity of GFP:MinE is the switching from the polar zone to midcell as in Figure 3(B), exhibiting three high-velocity peaks in micrometers per second. The average switching velocity is 2.17 ± 0.68 μm/s. This phenomenon reflects a topological specificity through the C-terminal function that is essential for midcell localization of MinE [29]. The RSML is the distance from the polar zone back to the midcell which corresponds to the cell length. The RSML was calculated to have an average of 2.39 μm, which is approximately half the cell length of 5.08 ± 0.82 μm.

A precise quantitative data analysis and consideration of the trajectory were possible via SPT. We can precisely measure the average oscillation period of a GFP:MinE cluster. One RSMT is defined as the time for the proteins to start to move from the midcell to the polar zone and then to revert to the midcell once again. Consequently, to move from the midcell to the opposite polar zone and revert to the midcell again would be two RSMT events or one period. As clearly seen in the Figure 3(B), at the abrupt change in the velocity referred to as the *switching velocity*, the velocity has a maximum value. The switching velocity is used to confirm the precise measurement of the period, *i.e.*, three switching velocities or three switching events define a period, as indicated by the black arrows shown in Figure 3(B). The measured

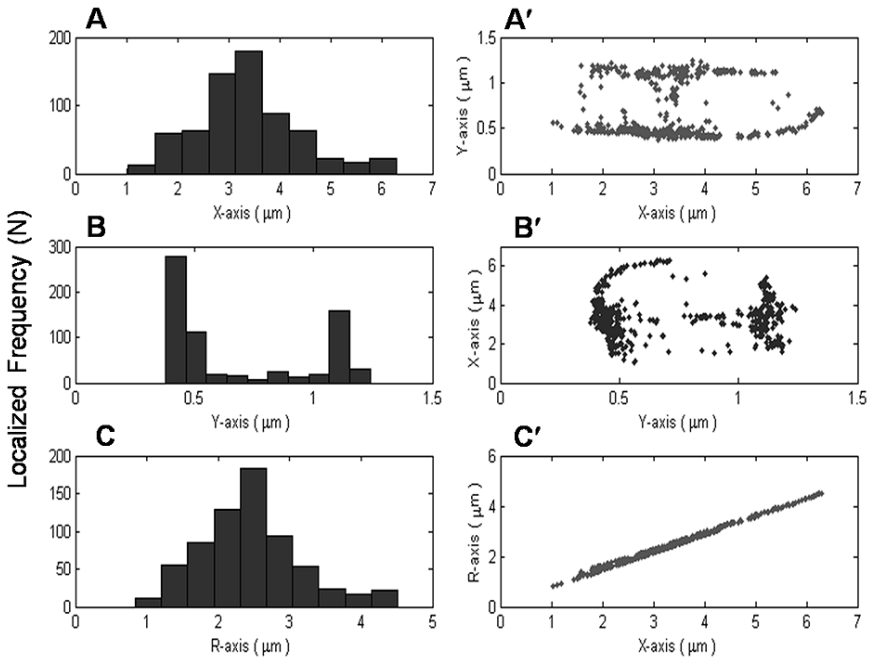

Fig. 4. Frequency histogram and positional scatterings of GFP:MinE localization. Figures 4(A), (B) and (C) are histograms that exhibit the localized frequency and patterns of GFP:MinE proteins present along the x, y and R axes respectively. Figures 4(A′), (B′) and (C′) show positional scatterings qualitatively exhibiting distributions of GFP:MinE on x-y, y-x and R-x, respectively.

oscillation period is 266.64 ± 122.29 seconds, with *E. coli* cell length of 5.08 ± 0.82 μm. Unlike the oscillation periods of MinD in which quite a number of data were provided [9,11,14,24,25], the period of MinE is rarely reported. To our knowledge, so far there has been only one report [13] that indicated the oscillation period of MinE (128 ± 39 sec). The difference is due to many causes and more experimental works are needed to draw conclusions regarding the oscillation period. Even in the GeneBank data base (http://ecogene.org/), there is no mention at all about MinE's oscillation period. This seems to indicate a subtle behavior of the MinE dynamics. Generally, the oscillation periods of Min proteins appear to depend on the cell length [13], the protein concentration [11], the temperature [33] and so on. Therefore, it is important to emphasize that having been able to obtain quantitative data is one of a new distinct reward of the SPT technique.

To support the above-mentioned explanations, we also demonstrated the interpretation can also be demonstrated by using a histogram and positional scatterings of GFP:MinE, as shown in Figure 4. Figure 4 shows the histograms demonstrating a localized frequency and patterns of GFP:MinE proteins that are found along the x, y and R axes in Figures 4(A), (B) and (C), respectively. Moreover, positional scatterings qualitatively exhibit distributions of GFP:MinE on x-y, y-x and R-x, as shown in Figures 4(A′), (B′) and (C′). The data were collected during a 600th time interval. Along the x-axis (or along the poles), it is clearly seen that MinE proteins mostly distribute and localize in the vicinity of the midcell. On the contrary, the region near the poles has a lower concentration of MinE, as previously reported [9–11,14]. To our knowledge, this is the first time that the time-averaged concentration of MinE has been experimentally and quantitatively revealed to be highest at the midcell, as qualitatively reported previously [28].

As a result of these quantifications, we are allowed to analyze the distribution of GFP:MinE positions along the major axis as shown in Figure 5. Here, a dotted straight line represents the data on positions while a dashed-dot line is the Gaussian distribution function fitting (GDF: $y = y_0 + \frac{A}{w\sqrt{\pi/2}} e^{-2(x-x_c)^2/w^2}$) with $R^2 = 0.995$. The middle position of the distribution is approximately 2.767 μm, as calculated from $x_{middle} = x_c - x_{min}$, $x_c = 3.269 \pm 0.027$ μm and $x_{min} = 0.502$ μm being determined from the minimum point of the MinE distribution position via GDF fitting and histogram, respectively. This graph quantitatively presents, for the first time, the distribution of MinE, though it was previously qualitatively reported [9–11,14] that MinE protein concentration was highest. at the midcell. Moreover, mathematical modeling and simulation results [24, 34–42] could also be validated and confirmed by using our experimental results. It is surprising, however, that no report has shown the precise space-time plot and associated trajectories. It may be important to point out that the GDF may imply that the MinE dynamics is mediated by a concentration-gradient-driven force of MinE or

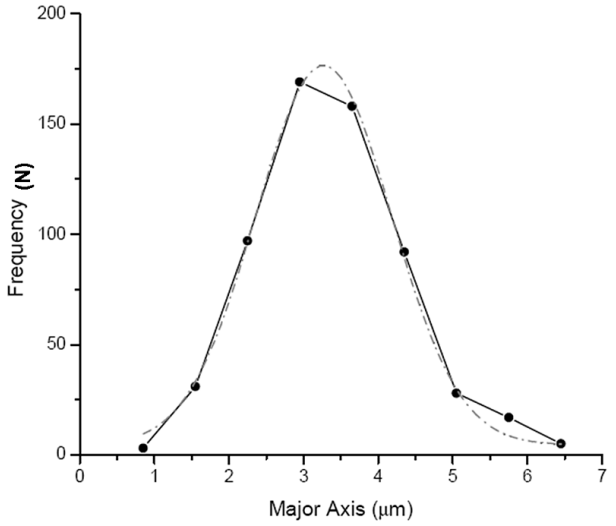

Fig. 5. Distribution of GFP:MinE positions along the major axis. The dotted straight line represents the cluster position data fitted to a Gaussian function (GDF: $y = y_0 + \frac{A}{w\sqrt{\pi/2}} e^{-2(x-x_c)^2/w^2}$) shown in a dashed-dot line with $R^2 = 0.995$. The middle position of the distribution is approximately 2.767 μm calculated from $x_{middle} = x_c - x_{min}$; $x_c = 3.269 \pm 0.027$ μm and $x_{min} = 0.502$ μm as determined from the minimum point of the MinE distribution position via a GDF fitting and a histogram, respectively.

more precisely the MinCDE system. It is possible that this graph may be used for determining where the midcell zone domain is or where the polar zone domain is. If so, it must be done with care and relevant biological considerations should be taken into account.

Having analyzed the trajectories and the velocities profiles, we found that the results revealed an oscillatory dynamic pattern between the polar zones. So far, at least it is qualitatively consistent with previous experimental and theoretical findings [33–37]. More importantly, using the extracted (x, y) allows us to precisely locate the positions of the MinE at a given time, portraying its trajectory. These precise positions can be used to calculate several physical quantities. One of the key characteristics of MinE is that assembles of GFP-MinE molecules are mostly concentrated at the midcell. These results are quite consistent with those of the previous reports [28]. We have learned from those previous studies that the dynamics of Min proteins at the polar zones are believed to correspond to polar zone growth by the formation of MinD polymerization at the cytoplasmic membrane [31, 32]. It is also possible that MinE may interact with itself or other Min proteins or cytoplasmic components in a complicated manner not yet well understood. During this state, as briefly mentioned in the introduction, MinE in E-ring activation of the ATPase activity of MinD:ATP molecules to undergo hydrolysis results in the release of MinD:ADP, MinC and MinE products from the membrane to the cytoplasm [8,30–32]. The MinE, thus, immediately sweeps MinD out of the midcell, allowing a Z-ring to form. The Z-ring assembly is spatially restricted to the midcell by nucleoid occlusion [4, 5] and by the MinCDE system [6,7].

Accordingly, with this SPT technique, we provided quantitative data on how local densities of MinE are distributed. The information will be of great value in predicting the specific site of localization and perhaps the reactions of MinE. Due to concerning the observed spatial inhomogeniety of MinE from previous findings [27, 36,41,43,44], it was theorized that it was due to the helical movement during the Min protein polymerization. Therefore, when we analyze vertical section of *E.coli*, many SPT spots will be seen mostly on the top and at the bottom, with somewhat constant intervals (data not shown). This phenomenon is expected to be clearly seen when using real time-three dimensional image capturing and reconstructing techniques, like confocal microscopy. Once again, on comparing these results with those from computation, good qualitative agreement was found.

With regards to Min protein dynamics both *in vitro* and *in silico*, a considerable number of experiments have been done. Computationally, several studies have been carried out with different reaction-diffusion models to explain these oscillations [35–40, 42]. It has also recently emerged that MinD forms helical filaments in living cells [24]; recent mathematical models [34,41] have attempted to include this feature. The model by Drew *et al.* [34] includes polymer growth from nucleation sites at the ends of the cell. Both of these models use continuous partial differential equations. The model by Pavin *et al.* [41] differs in that it is a three-dimensional stochastic model, but it does not yield the observed large-scale helical filaments. Incorporating the stochastic feature introduced into Min modeling is, nevertheless, likely to be important for systems of this type [27,36,41,43,44]. Although almost all previous findings were able to provide both qualitative and quantitative predictions of great interest, only qualitative ones were verified, mainly because of the lack of quantitative experimental data. Therefore, more a quantitative approach is greatly needed.

In summary, the SPT has made it possible to observe, both qualitatively and quantitatively, the MinE dynamics. All results are qualitatively found to agree with previously experimental and theoretical results. Moreover, more precise quantitative information regarding MinE dynamics has also been obtained, including specific positions, paths or trajectories, spatial distribution, switching and localization and oscillation periods. For example, our measured oscillation period is 266.64 $\pm$ 122.29 seconds, which is a new value for MinE oscillation period in bacteria for the strain RC1/pSY1083G with this size (5.08 $\pm$ 0.82 μm.). It is reasonable to say that the measurements performed, with SPT technique, are more accurate than those done by, say, eye-observed measurement in a 2D image sequence. However, the accuracy of this SPT technique may be subject to environmental factors. We believe that more data are needed to

reasonably specify the acceptable oscillation period of the MinE protein. An interesting characteristic of the time-evolution dynamics is the flight events that occur between the polar zones and midcell, a behavior that is still not well understood. With a further improved SPT technique, especially applications in 3D, the information to be gained may reflect some mechanisms, such as an obstruction of MinE by other mobile or immobile molecules or by other Min proteins, binding and obstruction by cellular components and so on. In terms of MinE localization, analysis of the cluster positions by using the SPT technique, of the patterns of localization and of the distribution along the cell length have not only been very well confirmed but other quantitative information related to MinE cluster positions have been revealed, as well.

Other questions of interest concerning MinE dynamics via SPT are, for example, the transport properties, the energy landscape, the fluctuation effects, the root-mean-square distance dynamics, the polymerization patterns and so on. We believe that the SPT technique will be widely applied to Min protein systems in the very near future like it has been used in other biological systems. Moreover, with improvements in the SPT technique, in data acquisition and in data analysis, this technique could become much more-accepted. The 3D, true to life results are, of course, what we strive for.

ACKNOWLEDGMENTS

We would like to greatly thank Prof. Lawrence Rothfield and Dr. Yu-Ling Shih (Department of Microbiology, University of Connecticut Health Health Center) for kindly providing *E. coli* RC1/pSY1083G [$\Delta min/P_{lac} - \Delta minC\Delta minD\Delta minE :: gfp$] for our use. Special thanks also go to Dr. Narin Nuttawut and Dr. Martin Howard for their fruitful discussions, to the Commission on Higher Education for the CHE-PhD-THA Program Scholarship to Paisan Kanthang and to the Development and Promotion of Science and Technology Talents Program Scholarship to Waipot Ngamsaad. This work was supported by The National Center for Genetic Engineering and Biotechnology (BIOTEC), The Thailand Research Fund (TRF), The Third World Academy of Sciences (TWAS) and The Institute of Science and Technology Development (ISTD).

REFERENCES

[1] F. J. Trueba, Arch. Microbiol. **131**, 55 (1982).
[2] J. Lutkenhaus and S. G. Addinall, Annu. Rev. Biochem. **66**, 93 (1997).
[3] L. Rothfield, S. Justice and J. Garcia-Lara, Annu. Rev. Genet. **33**, 423 (1999).
[4] C. L. Woldringh, E. Mulder, P. G. Huls and Vischer, Res. Microbiol. **142**, 309 (1991).
[5] W. Yu, X. Fau-Margolin and W. Margolin, Mol. Microbiol. **32**, 315 (1999).
[6] P. A. de Boer, R. E. Crossley and L. I. Rothfield, Cell **56**, 641 (1989).
[7] Y. L. Rothfield, L. Fau-Shih, G. Shih, Y. Fau-King and G. King, Cell **106**, 13 (2001).
[8] L. Rothfield, A. Taghbalout and Y. L. Shih, Nat. Rev. Microbiol. **3**, 959 (2005).
[9] Z. Hu and J. Lutkenhaus, Mol. Microbiol. **34**, 82 (1999).
[10] D. M. Raskin and P. A. de Boer, J. Bacteriol. **181**, 6419 (1999).
[11] D. M. Raskin and P. A. de Boer, Proc. Natl. Acad. Sci. U.S.A. **96**, 4971 (1999).
[12] J. Justice, S. Fau-Garcia-Lara, L. I. Garcia-Lara, J. Fau-Rothfield and L. I. Rothfield, Mol. Microbiol. **37**, 410 (2000).
[13] X. Fu, Y. L. Shih, Y. Zhang and L. I. Rothfield, Proc. Natl. Acad. Sci. U.S.A. **98**, 980 (2001).
[14] H. Hale, C. Fau-Meinhardt, P. A. Meinhardt, H. Fau-de Boer and P. A. de Boer **20**, 1563 (2001).
[15] M. V. Matz, A. F. Fradkov, Y. A. Labas, A. P. Savitsky, A. G. Zaraisky, M. L. Markelov and S. A. Lukyanov, Nat. Biotechnol. **17**, 969 (1999).
[16] R. Y. Tsien, Annu. Rev. Biochem. **67**, 509 (1998).
[17] H. Qian, M. P. Sheetz and E. L. Elson, Biophys. J. **60**, 910 (1991).
[18] M. J. Saxton and K. Jacobson, Annu. Rev. Biophys. Biomol. Struct. **26**, 373 (1997).
[19] C. Babcock, H. Fau-Chen, X. Chen, C. Fau-Zhuang and X. Zhuang, Biophys. J. **87**, 2749 (2004).
[20] D. Sage, F. R. Neumann, F. Hediger, S. M. Gasser and M. Unser, IEEE. Trans. Image. Process. **14**, 1372 (2005).
[21] Z. Kim Sy Fau-Gitai, A. Gitai Z Fau-Kinkhabwala, L. Kinkhabwala A Fau-Shapiro and W. E. Moener, Proc. Natl. Acad. Sci. U.S.A. **103**, 10929 (2006).
[22] J. Lutkenhaus, Annu. Rev. Biochem. (2007).
[23] S. L. Rowland, X. Fu, M. A. Sayed and Y. Zhang, W. R. Cook and L. I. Rothfield, J. Bacteriol. **182**, 613 (2000).
[24] T. Shih Yl Fau-Le, L. Le T Fau-Rothfield and L. Rothfield, Proc. Natl. Acad. Sci. U.S.A. **100**, 7865 (2003).
[25] J. Szeto, N. F. Eng, S. Acharya, M. D. Rigden and J. A. R. Dillon, Research in Microbiology **156**, 17 (2005).
[26] R. E. de Boer, P. Fau-Crossley, A. R. Crossley, R. Fau-Hand, L. I. Hand Ar Fau-Rothfield and L. I. Rothfield, EMBO J. **10**, 4371 (1991).
[27] D. Fange and J. Elf, PLoS Comput. Biol. **2**, e80 (2006).
[28] D. M. Raskin and P. A. de Boer, Cell **91**, 685 (1997).
[29] G. F. King, Y. L. Shih, M. W. Maciejewski, N. P. Bains, B. Pan, S. L. Rowland, G. P. Mullen and L. I. Rothfield, Nat. Struct. Biol. **7**, 1013 (2000).
[30] Z. Hu and J. Lutkenhaus, Mol Cell **7**, 1337 (2001).
[31] E. P. Hu, Z. Fau-Gogol, J. Gogol, E. Fau-Lutkenhaus and J. Lutkenhaus, Proc. Natl. Acad. Sci. U.S.A. **99**, 6761 (2002).
[32] R. Suefuji, K. Fau-Valluzzi, D. Valluzzi, R. Fau-Ray Chaudhuri and D. RayChaudhuri, Proc. Natl. Acad. Sci. U.S.A. **99**, 16776 (2002).
[33] A. Touhami, M. Jericho and A. D. Rutenberg, J. Bacteriol. **188**, 7661 (2006).
[34] M. J. Drew, D. Fau-Osborn, L. I. Osborn, M. Fau-Rothfield and L. I. Rothfield, Proc. Natl. Acad. Sci. U.S.A. **102**, 6114 (2005).
[35] M. Howard, A. D. Rutenberg and S. de Vet, Phys. rev.

lett. **87**, 278102.1 (2001).
[36] A. D. Howard, M. Fau-Rutenberg and A. D. Rutenberg, Phys. Rev. Lett. **90**, 128102 (2003).
[37] K. C. Huang, Y. Meir and N. S. Wingreen, Proc. Natl. Acad. Sci. U.S.A. **100**, 12724 (2003).
[38] K. Kruse, Biophys. J. **82**, 618 (2002).
[39] H. Meinhardt and P. A. de Boer, Proc Natl. Acad. Sci. U.S.A. **98**, 14202 (2001).
[40] C. Modchang, P. Kanthang, W. Triampo, N. Ngamsaad, N. Nattawut and I. M. Tang, J. Korean Phys. Soc. **46**, 1031 (2005).
[41] N. Pavin, H. C. Paljetak and V. Krstic, Phys. Rev. E. Stat. Nonlin. Soft. Matter. Phys. **73**, 021904 (2006).
[42] W. Ngamsaad, W. Triampo, P. Kanthang, I. M. Tang, N. Nattawut and C. Modchang, J. Korean Phys. Soc. **46**, 1025 (2005).
[43] R. A. Kerr, H. Levine, T. J. Sejnowski and W. J. Rappel, Proc. Natl. Acad. Sci. U.S.A. **103**, 347 (2006).
[44] F. Tostevin and M. Howard, Phys. Biol. **3**, 1 (2006).